Published in final edited form as:
J Biomech. 2010 November 16; 43(15): 3028–3034. doi:10.1016/j.jbiomech.2010.06.031.

The effect of cement creep and cement fatigue damage on the micromechanics of the cement-bone interface

Daan Waanders[1], **Dennis Janssen**[1], **Kenneth A. Mann**[2], and **Nico Verdonschot**[1,3]

[1]Orthopaedic Research Laboratory, Radboud University Nijmegen Medical Centre, Nijmegen, The Netherlands [2]Department of Orthopaedic Surgery, SUNY Upstate Medical University, Syracuse, NY, USA [3]Laboratory for Biomechanical Engineering, University of Twente, Enschede, The Netherlands

Abstract

The cement-bone interface provides fixation for the cement mantle within the bone. The cement-bone interface is affected by fatigue loading in terms of fatigue damage, or micro cracks, and creep, both mostly in the cement. This study investigates how fatigue damage and cement creep separately affect the mechanical response of the cement-bone interface at various load levels in terms of plastic displacement and crack formation. Two FEA models were created, which were based on micro-computed tomography data of two physical cement-bone interface specimens. These models were subjected to tensile fatigue loads with four different magnitudes. Three deformation modes of the cement were considered; ‘only creep’, ‘only damage’ or ‘creep and damage’. The interfacial plastic deformation, the crack reduction as a result of creep and the interfacial stresses in the bone were monitored. The results demonstrate that, although some models failed early, the majority of plastic displacement was caused by fatigue damage, rather than cement creep. However, cement creep does decrease the crack formation in the cement up to 20%. Finally, while cement creep hardly influences the stress levels in the bone, fatigue damage of the cement considerably increases the stress levels in the bone. We conclude that at low load levels the plastic displacement is mainly caused by creep. At moderate to high load levels, however, the plastic displacement is dominated by fatigue damage and is hardly affected by creep, although creep reduced the number of cracks in moderate to high load region.

Keywords

Finite element; fatigue; bone; bone cement; interface

Correspondence: Daan Waanders, Orthopaedic Research Lab, Radboud University Nijmegen Medical Centre, P.O. Box 9101, 6500 HB Nijmegen, The Netherlands, T: +31 24 3617379, F: +31 24 3540555, d.waanders@orthop.umcn.nl.

CONFLICT OF INTEREST STATEMENT

None of the authors have financial or personal relationships with other people or organizations that could inappropriately influence or bias the currently presented work.

1. INTRODUCTION

The cement-bone interface provides fixation for cemented implants within bone. The interface is formed during polymethymethacrylate (PMMA) cement injection, when the cement is pressurized into the bone cavities. This results in a highly variable interlock between the bone and cement with a complex morphology and mechanical properties (Wang et al., 2010; Mann et al., 2008; Maher and McCormack, 1999). Experiments with cement-bone interface specimens have shown that the interface degrades over time by fatigue loading (Yang et al., 2010; Mann et al., 2009; Waanders et al., 2009; Kim et al., 2004a). Under the influence of dynamic loading, creep and fatigue damage occurs in the cement and bone, causing a reduced stiffness and increased motion at the interface. Furthermore, experiments have shown that creep and fatigue cracking at the cement-bone interface occur mainly in the cement, rather than in the bone (Yang et al., 2010; Mann et al., 2009; Waanders et al., 2009; Kim et al., 2004b).

Studies on the creep behaviour of PMMA bulk cement have indicated that creep effectively attenuates stress peaks in the cement mantle (Verdonschot and Huiskes, 1997; Lu and McKellop, 1997; Norman et al., 2001), which reduces fatigue cracking of the cement. Since it is experimentally impossible to delineate how creep and fatigue damage interact at the cement-bone interface it is unknown which one affects the interface integrity the most. Finite Element Analysis (FEA) make this possible, but numerical studies in which fatigue failure of the cement-bone interface was investigated have not studied the relatively contribution of creep and fatigue damage (Perez and Palacios, 2010; Waanders et al., 2009).

In the current study, we assessed the relative effect of creep and fatigue in micromechanical FEA-models of cement-bone interface specimens and tried to answer the following questions: (1) How do cement creep and cement fatigue damage independently affect the micromechanical response of the cement-bone interface at various load levels, and how do these two phenomena interact in a combined model?; (2) Does cement creep influence fatigue crack formation in the cement? (3) How do cement creep, cement fatigue damage or a combination of both affect the stress levels in the bone?

2. METHODS

Two rectangular-prism shaped FEA-models (~8×4×8mm^3) were created using micro-CT scans (12μm isotropic resolution) of two physical cement-bone interface specimens that were sectioned from laboratory-prepared cemented total hip replacements (Waanders et al., 2009). Each model comprised two components, bone and cement (Figure 1), and the two models had substantial differences regarding bone morphology. The bone model comprised the bony tissue of the cement-bone interface, the interfacial gaps and lacunar spaces. A voxel mesh of the bone model was automatically created by segmentation of the micro-CT data using MIMICS 11.0 (Materialise, Leuven, Belgium), based on the image grey scales, which ranged from −1,000 to 3,071 (bone 1,000 to 3,071; gaps −1,000 to 100) (Janssen et al., 2009). Grooves that were not selected during the first segmentation were segmented manually. Next, a triangular surface mesh was generated from the voxel mesh using a 6×6×6 voxel reduction with smoothing (Leung et al., 2008). The smoothed meshes were assessed on their accuracy in which deficiencies were solved manually. The surface mesh was subsequently converted to a tetrahedral 3D solid mesh (PATRAN 2005r2, MSC Software Corporation, Santa Ana, CA, USA) and mapped back into the micro-CT data, after which the weighted average of the grey scale was calculated for each element. Subsequently, an erosion algorithm was applied to the solid mesh to model the interfacial gaps between the bone and the cement (Waanders et al., 2009). The morphology of the cement was based on the non-eroded mesh of the bone.

The contact interface between the bone and cement was assumed to be unbonded (Lucksanasombool et al., 2003; Janssen et al., 2009; Goto et al., 2009). Frictional contact between the bone and cement was modelled using a double-sided node-to-surface algorithm (MSC Marc 2007r1, MSC Software Corporation, Santa Ana, CA, USA) with a friction coefficient of 0.3 (Janssen et al., 2008). In total, specimen 1 consisted of 462,102 elements and 109,568 nodes while specimen 2 consisted of 219,664 elements and 53,499 nodes.

The initial material properties of the bone and cement were considered to be linear elastic (Leung et al., 2006). The averaged grey values of the bone elements were converted to HA-density values using a calibration phantom. Although some large BaSO4 particles resulted in local beam hardening artefacts in the cement, this did not affect the grey values in the bone. The Young's modulus (*E*) was assumed to be linearly dependent on the HA-density (Lotz et al., 1991), resulting in Young's moduli ranging from 0.1 to 20,000MPa. The cement was assumed to have a constant Young's modulus of 3,000MPa (Lewis, 1997). The Poisson's ratio was set to 0.3 for both the bone and the cement.

Both specimens were virtually loaded for a total of 50,000 cycles, with an assumed frequency of 1Hz, at four different tensile fatigue load levels: 0.1, 0.5, 1.0 and 2.0MPa. By means of a custom written FEA-algorithm that separately simulated fatigue damage and creep to the cement (Stolk et al., 2004), we were able to simulate the time dependent behaviour of the cement. The bone was assumed to remain unimpaired, since previous studies have demonstrated that the majority of the damage occurs in the cement and not in the bone (Waanders et al., 2009; Mann et al., 2009). For each load level, we simulated either *'only fatigue damage'*, *'only creep'*, or both *'creep and fatigue damage'* occurring to the cement (total of 24 simulations).

The utilized FEA-algorithm (Stolk et al., 2004) calculated the element deformation, $\{\varepsilon\}$, as: $\{\varepsilon\} = [S]\{\sigma\} + \{\varepsilon^c\}$. Fatigue damage was implemented in the compliance matrix $[S]$ in which for each of the three principal stress directions a damage parameter (D) indicated whether an element was cracked ($D = 1$). A crack was simulated by locally reducing the stiffness to 0.1MPa perpendicular to the corresponding maximum principal stress direction. Damage was calculated as:

$$D = \left(\frac{n}{Nf}\right)^{3.92} \quad where: \quad 0 \le D \le 1$$

in which *n and Nf* were the number of loading cycles and the fatigue life, respectively. The fatigue life (Nf) was determined based on the maximum principal stress (σ):

$$\sigma = -4.736 \cdot \mathbf{log}(Nf) + 37.8$$

Creep was implemented in the creep strain tensor $\{\varepsilon^c\}$ which was dependent on the scalar ε^c defined as: $\varepsilon^c = 7.982 \cdot 10^{-7} \cdot n^{0.4113 - 0.116 \cdot \mathbf{log}(\sigma)} \cdot \sigma^{1.9063}$ (Verdonschot and Huiskes, 1995).

For each model the plastic displacement was determined to study the effect of creep and damage in the interface deformation. The plastic displacement was defined as the difference between the total displacement and elastic displacement. If the plastic displacement exceeded 0.1mm the interface was assumed to be failed (Waanders et al., 2009).

During the simulations the total crack volume (V_{cr}) of the cement was monitored. The total crack volume was defined as the ratio between total volume of cracked elements and the

total cement volume: $V_{cr}=\frac{1}{3 \cdot V_{tot}} \cdot \sum_{i=1}^{N_{ele}} n_i \cdot V_i$. In this definition V_{tot}, n_i, and V_i were the total volume of the bulk cement, the number of cracks in each element ($0 \leq n_i \leq 3$) and the element volume, respectively.

To assess whether cement creep influences fatigue crack formation in the cement, the total crack volumes of the *'only damage'* and *'creep and damage'* were compared. For each load the reduction of cracks by creep was determined by: $\left(1 - \frac{V_{cr\&dam}}{V_{dam}}\right) \cdot 100\%$.

The stress levels in the bone were determined for the 0.1 and 1.0MPa loads of specimen 1, and the 0.1 and 0.5MPa loads for specimen 2. Different maximum stress levels for specimen 1 and 2 were chosen, since specimen 1 was approximately twice as stiff as specimen 2 (Waanders et al., 2009). At the beginning and at the end of the simulation, Von Mises stresses were determined only for the group of elements that lied at the contact interface (Figure 2). All the stresses were normalized for this group of elements by dividing by the applied apparent stress, $\frac{\sigma_{VM}}{\sigma_{app}}$. Subsequently, the normalized stresses were divided in 20 groups ranging from $0 \leq \frac{\sigma_{VM}}{\sigma_{app}} \leq 10[-]$ and one group $\frac{\sigma_{VM}}{\sigma_{app}} > 10[-]$.

3. RESULTS

There was a wide range of responses from the 24 tension fatigue simulations (Figure 3). Six simulations led to early failure of the specimens (plastic displacement>0.1mm). With the exception of the failed specimens, all the simulations showed the first two stages of the classical three-phase creep response. All simulations in which *'only creep'* was considered as a plastic deformation mode did not result in failed specimens.

For the specimens that were subjected to a 0.1MPa apparent load, creep was over the long term (N=50,000) the dominant factor in the time dependent plastic displacement (Figure 3, 4). At the higher load levels, damage contributed much more to interface deformation than creep. Simulations that included '*creep and fatigue damage*' always resulted in the greatest plastic displacement.

Creep considerably reduced the formation of cracks in the cement (Figure 5). At N=50,000, the crack volume was reduced up to 20% with respect to the situation in which damage was considered to be the only deformation mode. Due to the low amount of cement damage, the simulations at a 0.1MPa load showed a very inconsistent response.

There were distinct differences in Von Mises stresses in the bone. Directly after loading with an apparent stress of 0.1MPa, ~88% and ~80% of the total interface volume had a $\frac{\sigma_{VM}}{\sigma_{app}} \leq 1$, for specimen 1 and 2, respectively (Figure 6). When loaded to higher load levels, the relative stresses at the bony interface were much higher. When specimen 1 was loaded to 1.0MPa, ~35% of the interface volume had a $\frac{\sigma_{VM}}{\sigma_{app}} \leq 1$ and ~11% a $\frac{\sigma_{VM}}{\sigma_{app}} > 10$. When specimen 2 was loaded to 0.5MPa, ~53% of the interface volume had a $\frac{\sigma_{VM}}{\sigma_{app}} \leq 1$ and ~10% a $\frac{\sigma_{VM}}{\sigma_{app}} > 10$.

When loaded to 0.1MPa, cement creep and or fatigue damage had limited influence on the bone stress level for specimen 1 and specimen 2 after N=50,000 (Figure 7). However, when

the specimens were subjected to higher loads there was a decrease in the volume with relative low bone stresses, $\frac{\sigma_{VM}}{\sigma_{app}} \leq 1$, and increase the volume with relative high bone stresses, $\frac{\sigma_{VM}}{\sigma_{app}} > 1$ (Figure 7). While the situations in which *'only creep'* was considered showed minor increases in bone stress level compared to the initial bone stress level (N=1), fatigue damage resulted in a considerable increase in bone stress level. Comparison of the *'creep and damage'* with the *'only damage'* situations showed limited differences between the two; this demonstrates the minor influence of creep on the bone stress level (Figure 8).

4. DISCUSSION

In the current study we sought to gain insight in the relative contributions of cement creep and cement fatigue crack formation on the cement damage and micromechanical response of the cement-bone interface. We used these two deformation modes to study the consequences on the cement-bone interfacial plastic deformation, crack formation in the cement and interfacial stress levels in the bone.

Our results show that at almost all load levels, the majority of the time dependent plastic displacement found at the cement-bone interface was due to the formation of fatigue cracks which arose at the contact interface and subsequently progressed further into the bulk cement. When subjected to low stresses, however, the relative contribution of creep increased. The combined models in which both creep and fatigue cracking were simulated showed that creep had virtually no additional effect on the plastic response of the interface compared to the case with simulated cement fatigue cracking only.

Although the effect on the deformation of the interface was minimal, creep did reduce fatigue crack formation. The extent of this effect depended both on stress level and specimen morphology, but was most effective at lower stress levels since high stresses resulted in early failure of the specimen not giving creep the opportunity to decrease the crack formation effectively. This suggests that at higher external stresses, creep is not capable of relieving peak cement stresses to such an extent that fatigue crack formation is attenuated.

Fatigue cracking of the cement increased the stresses in the bone at the interface, while cement creep did not appear to have a considerable effect on bone stresses. Most likely the load transfer was altered due to cement cracking, enabling loads to be transferred over a different contact area, thereby increasing local bone stresses. Regardless, the increase of high stresses in the bone, the cracking of the cement will also reduce the global stiffness of the cement-bone interface (Mann et al., 2009; Waanders et al., 2009). This, subsequently, results in large motions at the cement-bone interface (Figure 3) and of the complete cement mantle within the femur (Mann et al., 2010).

While cement creep was able to reduce the number of fatigue cracks in the cement, it was not capable of reducing the stresses near the cement-bone interface. In contrast, previous studies have shown that creep does reduce the stresses at the stem-cement interface (Lu and McKellop, 1997; Norman et al., 2001) and in the cement mantle (Verdonschot and Huiskes, 1997). Several phenomena might explain this discrepancy. First of all, the bone stresses might remain rather high due to the morphology of the cement-bone interface which is much more convoluted than the stem-cement interface in terms of more interfacial gaps (Miller et al., 2010), less relative contact area (Mann et al., 2008) and higher interdigitation (Janssen et al., 2009). This might subsequently result in much higher peak stresses in the cement which is more sensitive to cracking than creeping (Stolk et al., 2004). Cement cracking as a dominant failure type can also be seen at other convoluted interfaces such as the stem-

cement interface where there is much more wear debris after debonding for rough stems than for polished stems (Scheerlinck and Casteleyn, 2006). Besides the physical morphology, the applied boundary conditions might also be responsible for the fact that the bone stresses did not reduce as a consequence of creep. In the current study, a constant apparent stress was applied which remained constant during the whole situation, basically not giving the local stresses the opportunity to decrease to zero. If initially a fixed displacement would have been applied, which would have been remained constant during the whole simulation, stresses would be able to spread and level out in time. Moreover, in the studies of Lu and McKellop (1997) and Verdonschot and Huiskes (1997) the stresses were analyzed utilizing models of complete cemented hip reconstructions. In contrast to the current micro models of the cement-bone interface, complete models of cemented hip reconstructions have restrictions in deformation of the interface. This makes stresses able to redistribute in time (Moreo et al., 2006), due to for example creep.

Our study was limited with respect to material property assumptions, external loads, and interface morphology. The utilized FEA-models were idealized and focussed on the in-vitro failure of the cement-bone interface, hence biological responses were not considered, what is in conflict to what happens in-vivo (Mann et al., 2010; Miller et al., 2010; Gardiner and Hozack, 1994). The creep and fatigue properties were used for a single type of PMMA cement only, while the creep and fatigue damage response may vary over the different types of bone cements that are currently available on the orthopaedic market. Trabecular bone that is subjected to cyclic loads also shows fatigue damage (Dendorfer et al., 2009; Cotton et al., 2005). However, since previous experiments have demonstrated that bone fatigue cracking was much lower in magnitude compared to cement damage (Mann et al., 2009; Waanders et al., 2009), this was not simulated. How fatigue damage in the bone could affect the simulated plastic deformation in the cement bone interface is unknown. The plastic deformation could simply increase, but on the other hand, the stresses at the contact interface could also be distributed more evenly, resulting in less fatigue damage. In addition, although the effect of different load levels was analyzed, the models were loaded in the tensile direction only. Whether in shear the same quantitative findings would be obtained is unknown. Previous studies have shown that different loading directions can result in different mechanical responses, such as crack patterns (Mann et al., 2009; Waanders et al., 2009; Moreo et al., 2006; Mann et al., 2001; Yang et al., 2010). Finally, only two interface morphologies were included in the current study. However, as previous studies have indicated that the micromechanical response depends on interface morphology (e.g. contact area, cement penetration depth) (Waanders et al., 2010; Mann et al., 2008), we chose two specimens with substantial morphological differences. In-vivo phenomena that would influence the morphology of the cement-bone interface were also accounted for, since during the generation of the cement-bone interface specimens in-vivo conditions, like endosteal bleeding, were reproduced (Mann et al., 2008). The thickness of the cement mantle adjacent to the cement-bone interface was modelled by a 1.0mm thick layer of cement at the bottom of the FEA-models. However, the adjacent layer of cement has negligible effects on the mechanical fatigue response of the cement-bone interface (Mann et al., 2009; Waanders et al., 2009).

The current study is unique in the sense that cement creep and fatigue damage were separated to study their relative contributions to the micromechanical response of the cement-bone interface subjected to repetitive loads. The current results may be useful in the synthesis of new bone cement formulations. For instance, our finding that fatigue crack formation is responsible for the majority of the plastic deformation of the cement-bone interface indicates that, if one is interested in improving the dynamic response of the interface, the fatigue properties of cement should be improved upon, rather than modifying the creep properties. Moreover, improved fatigue resistance of the cement may confine the

increase of interfacial stresses. If the goal is to reduce the quantity of fatigue cracks in the cement, one could consider modifying the cement to allow more creep.

Based on the findings in the current study we conclude that: (1) When the cement-bone interface is subjected to low stresses, the plastic interface displacement is mostly caused by cement creep, while at higher loads cement fatigue cracking is unambiguously the dominant factor; (2) cement creep is able to decrease the crack formation in the cement up to 20%; and (3) cement creep is not capable of decreasing the stress levels in the bone with respect to the initial state and cement fatigue damage only results in an increase in bone stresses.

Acknowledgments

This work was funded by the NIH grant AR42017.

Reference List

1. Cotton JR, Winwood K, Zioupos P, Taylor M. Damage rate is a predictor of fatigue life and creep strain rate in tensile fatigue of human cortical bone samples. J.Biomech.Eng. 2005; 127:213–219. [PubMed: 15971698]
2. Dendorfer S, Maier HJ, Hammer J. Fatigue damage in cancellous bone: an experimental approach from continuum to micro scale. J.Mech.Behav.Biomed.Mater. 2009; 2:113–119. [PubMed: 19627813]
3. Gardiner RC, Hozack WJ. Failure of the cement-bone interface. A consequence of strengthening the cement-prosthesis interface? J.Bone Joint Surg.Br. 1994; 76:49–52. [PubMed: 8300681]
4. Goto K, Kawanabe K, Kowalski R, Baker D, Nakamura T. Bonding ability evaluation of bone cement on the cortical surface of rabbit's tibia. J.Mater.Sci.Mater.Med. 2009 in press.
5. Janssen D, Mann KA, Verdonschot N. Micro-mechanical modeling of the cement-bone interface: The effect of friction, morphology and material properties on the micromechanical response. J.Biomech. 2008; 41:3158–3163. [PubMed: 18848699]
6. Janssen D, Mann KA, Verdonschot N. Finite element simulation of cement-bone interface micromechanics: a comparison to experimental results. J.Orthop.Res. 2009; 27:1312–1318. [PubMed: 19340877]
7. Kim DG, Miller MA, Mann KA. A fatigue damage model for the cement-bone interface. J.Biomech. 2004a; 37:1505–1512. [PubMed: 15336925]
8. Kim DG, Miller MA, Mann KA. Creep dominates tensile fatigue damage of the cement-bone interface. J.Orthop.Res. 2004b; 22:633–640. [PubMed: 15099645]
9. Leung SY, Browne M, New AM. Smooth surface micro finite element modelling of a cancellous bone analogue material. Proc.Inst.Mech Eng H. 2008; 222:145–149. [PubMed: 18335725]
10. Leung SY, New A, Browne M. Modelling the mechanics of the cement-bone interface. J.Biomech. 2006; 39:S515.
11. Lewis G. Properties of acrylic bone cement: state of the art review. J.Biomed.Mater.Res. 1997; 38:155–182. [PubMed: 9178743]
12. Lotz JC, Gerhart TN, Hayes WC. Mechanical properties of metaphyseal bone in the proximal femur. J.Biomech. 1991; 24:317–329. [PubMed: 2050708]
13. Lu Z, McKellop H. Effects of cement creep on stem subsidence and stresses in the cement mantle of a total hip replacement. J.Biomed.Mater.Res. 1997; 34:221–226. [PubMed: 9029302]
14. Lucksanasombool P, Higgs WA, Ignat M, Higgs RJ, Swain MV. Comparison of failure characteristics of a range of cancellous bone-bone cement composites. J.Biomed.Mater.Res.A. 2003; 64:93–104. [PubMed: 12483701]
15. Maher SA, McCormack BA. Quantification of interdigitation at bone cement/cancellous bone interfaces in cemented femoral reconstructions. Proc.Inst.Mech Eng H. 1999; 213:347–354. [PubMed: 10466365]
16. Mann KA, Miller MA, Cleary RJ, Janssen D, Verdonschot N. Experimental micromechanics of the cement-bone interface. J.Orthop.Res. 2008; 26:872–879. [PubMed: 18253965]

17. Mann KA, Miller MA, Race A, Verdonschot N. Shear fatigue micromechanics of the cement-bone interface: An in vitro study using digital image correlation techniques. J.Orthop.Res. 2009; 27:340–346. [PubMed: 18846550]

18. Mann KA, Miller MA, Verdonschot N, Izant TH, Race A. Functional interface micromechanics of 11 en-bloc retrieved cemented femoral hip replacements. Acta Orthop. 2010; 81:308–317. [PubMed: 20367421]

19. Mann KA, Mocarski R, Damron LA, Allen MJ, Ayers DC. Mixed-mode failure response of the cement-bone interface. J.Orthop.Res. 2001; 19:1153–1161. [PubMed: 11781018]

20. Miller MA, Eberhardt AW, Cleary RJ, Verdonschot N, Mann KA. Micromechanics of postmortem-retrieved cement-bone interfaces. J.Orthop.Res. 2010; 28:170–177. [PubMed: 19658167]

21. Moreo P, Perez MA, Garcia-Amar JM, Doblare M. Modelling the mixed-mode failure of cement-bone interfaces. Engineering Fracture Mechanics. 2006; 73:1379–1395.

22. Norman TL, Thyagarajan G, Saligrama VC, Gruen TA, Blaha JD. Stem surface roughness alters creep induced subsidence and 'taper-lock' in a cemented femoral hip prosthesis. J.Biomech. 2001; 34:1325–1333. [PubMed: 11522312]

23. Perez MA, Palacios J. Comparative finite element analysis of the debonding process in different concepts of cemented hip implants. Ann.Biomed Eng. 2010; 38:2093–2106. [PubMed: 20232148]

24. Scheerlinck T, Casteleyn PP. The design features of cemented femoral hip implants. J.Bone Joint Surg.Br. 2006; 88:1409–1418. [PubMed: 17075082]

25. Stolk J, Verdonschot N, Murphy BP, Prendergast PJ, Huiskes R. Finite element simulation of anisotropic damage accumulation and creep in acrylic bone cement. Engineering Fracture Mechanics. 2004; 71:513–528.

26. Verdonschot N, Huiskes R. Dynamic creep behavior of acrylic bone cement. J.Biomed.Mater.Res. 1995; 29:575–581. [PubMed: 7622542]

27. Verdonschot N, Huiskes R. Acrylic cement creeps but does not allow much subsidence of femoral stems. J.Bone Joint Surg.Br. 1997; 79:665–669. [PubMed: 9250762]

28. Waanders D, Janssen D, Mann KA, Verdonschot N. The mechanical effects of different levels of cement penetration at the cement-bone interface. J.Biomech. 2010; 43:1167–1175. [PubMed: 20022010]

29. Waanders D, Janssen D, Miller MA, Mann KA, Verdonschot N. Fatigue creep damage at the cement-bone interface: an experimental and a micromechanical finite element study. J.Biomech. 2009; 42:2513–2519. [PubMed: 19682690]

30. Wang JY, Tozzi G, Chen J, Contal F, Lupton C, Tong J. Bone-cement interfacial behaviour under mixed mode loading conditions. J Mech Behav Biomed Mater. 2010; 3:392–398. [PubMed: 20416553]

31. Yang DT, Zhang D, Arola D. Fatigue of the bone/cement interface and loosening of tatal joint replacements. International Journal of Fatigue. 2010 in Press.

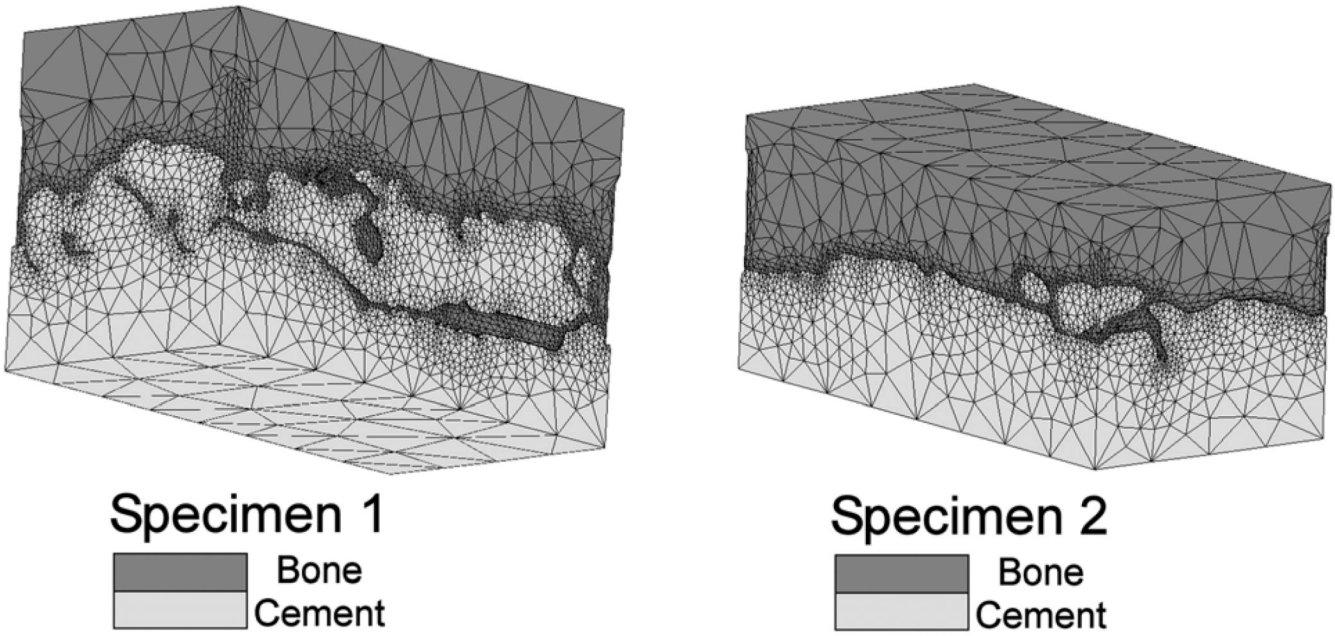

Figure 1.
The two cement-bone specimens were created from micro-CT data sets of laboratory-prepared cemented proximal femurs. Cement penetration into the bone varied over the two models; 2.2mm and 1.7mm for model 1 and model 2, respectively (Waanders et al., 2010)A tensile fatigue load was applied to one of the nodes in the top plane of the bone. All the other nodes in that particular plane were tied to that node to prevent the plane from tilting. The bottom of the cement was fixed.

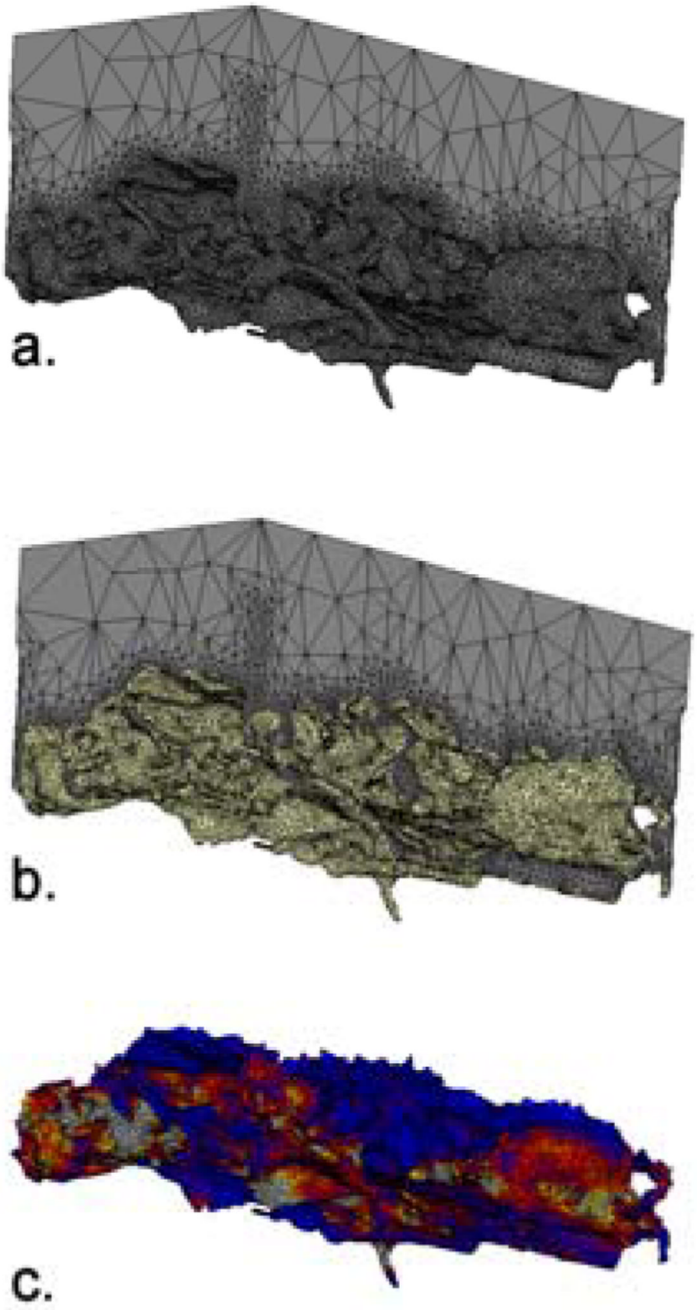

Figure 2.

Approach used to determine the stress level in the bone: From the bone model (a) all the nodes at the bone-cement contact interface were identified and the elements that shared one of the selected nodes was selected (b). The Von Mises stresses in those elements (c) were subsequently normalized by dividing them by the applied apparent stress, $\frac{\sigma_{VM}}{\sigma_{app}}$.

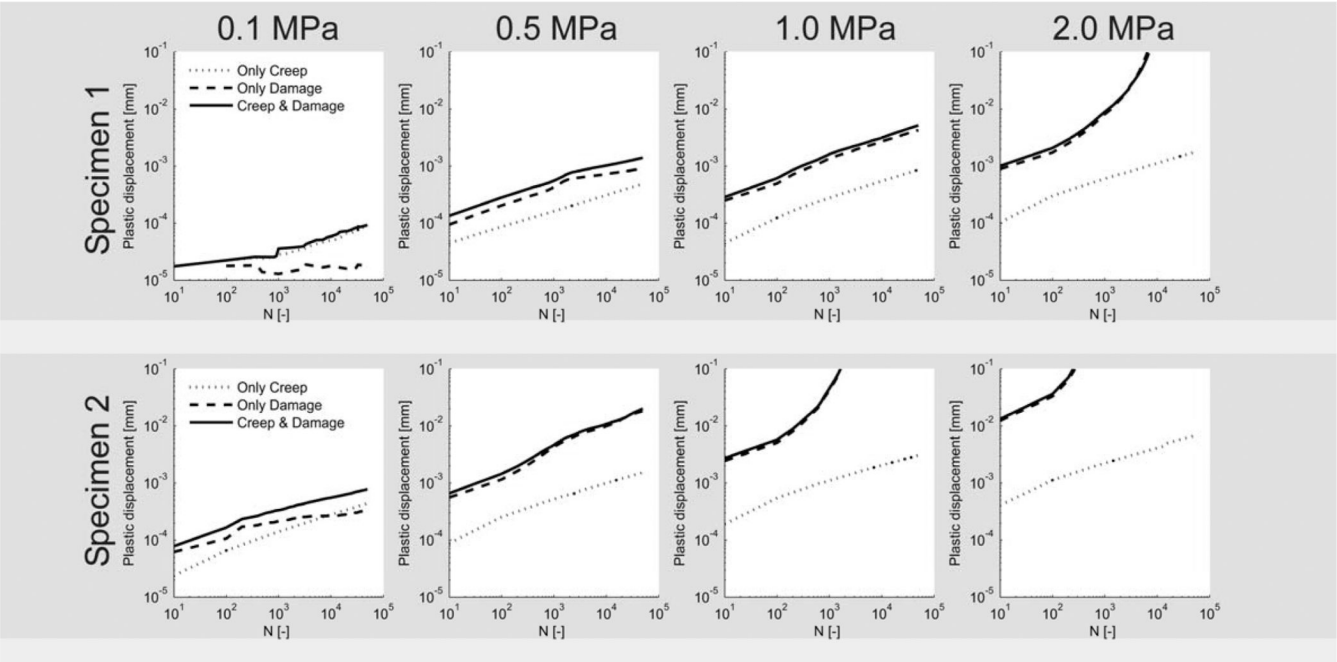

Figure 3.

Tensile fatigue responses of all 24 simulations. With the exception of the failed specimens (plastic displacement > 0.1mm) all simulations showed a logarithmic behaviour in which the simulations with *'creep and damage'* always resulted in the highest plastic displacement.

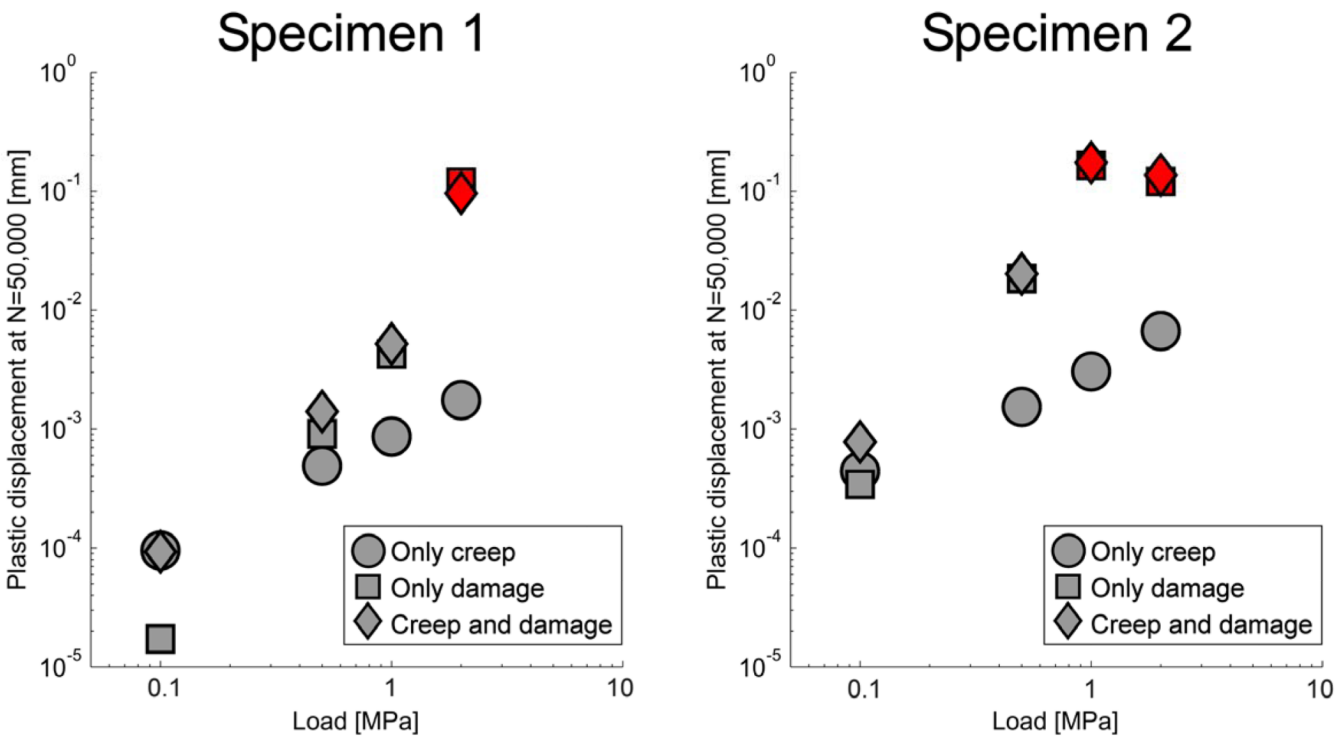

Figure 4.

Plastic displacement at N=50,000 load cycles. Red markers indicate that the specimen failed before reaching N=50,000 load cycles. While specimen 1 only failed with a 2.0MPa apparent load, specimen 2 failed as well at 1.0 as at 2.0MPa. The simulations in which *'only creep'* was considered remained intact.

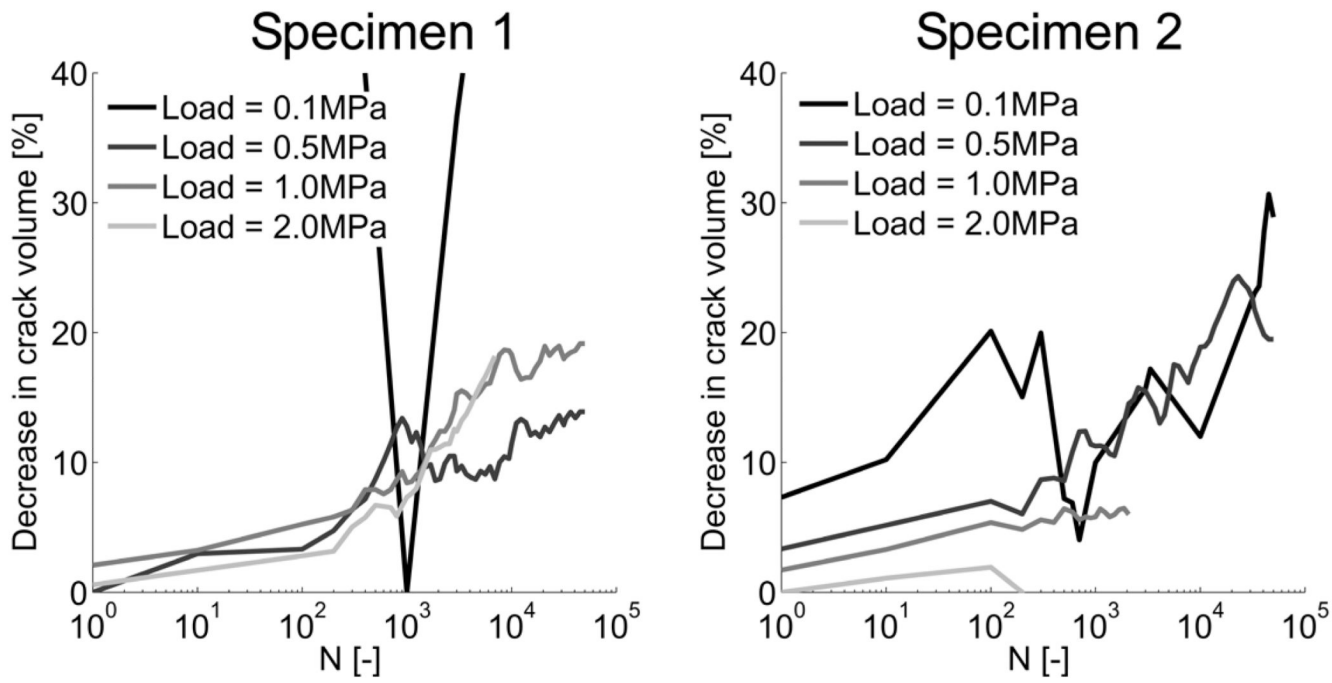

Figure 5.

The progression of decrease in cement crack volume due to cement creep in time (number of loading cycles) for both specimens. When *'creep and damage'* were considered as deformation modes, the crack volume was reduced up to 20% with respect to *'only damage'* situation. The unsteady response of the 0.1MPa simulations can be explained by the very low crack volume that occurred in the *'only damage'* and *'creep and damage'* response. For this stress level, a small change in crack volume resulted in relatively large decreases in crack volume. When specimen 2 was loaded to 2.0MPa, there was a very small effect of cement creep. However, at this load the specimen also failed in less than 200 loading cycles (Figure 3).

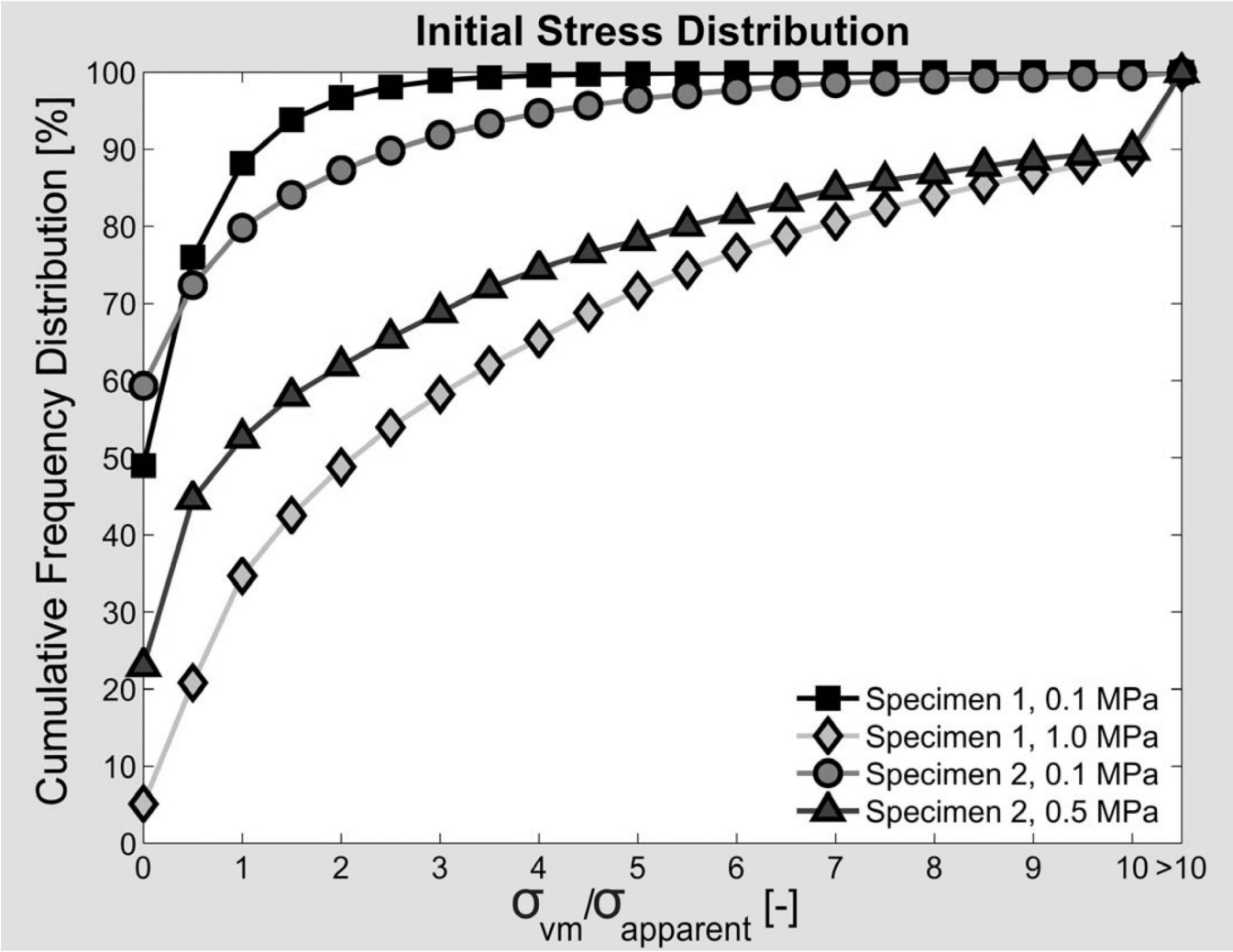

Figure 6.

Cumulative frequency distribution for $\frac{\sigma_{VM}}{\sigma_{app}}$ in the bone directly after loading (N=1) with different apparent stresses for specimen 1 and specimen 2. An apparent stress of 0.1 MPa resulted in ~88% and ~80% interface volume with $\frac{\sigma_{VM}}{\sigma_{app}} \leq 1$ for specimen 1 and specimen 2, respectively. When the two specimens were loaded to higher load levels, more than 10% of the total interface volume had a normalized stress of $\frac{\sigma_{VM}}{\sigma_{app}} > 10$.

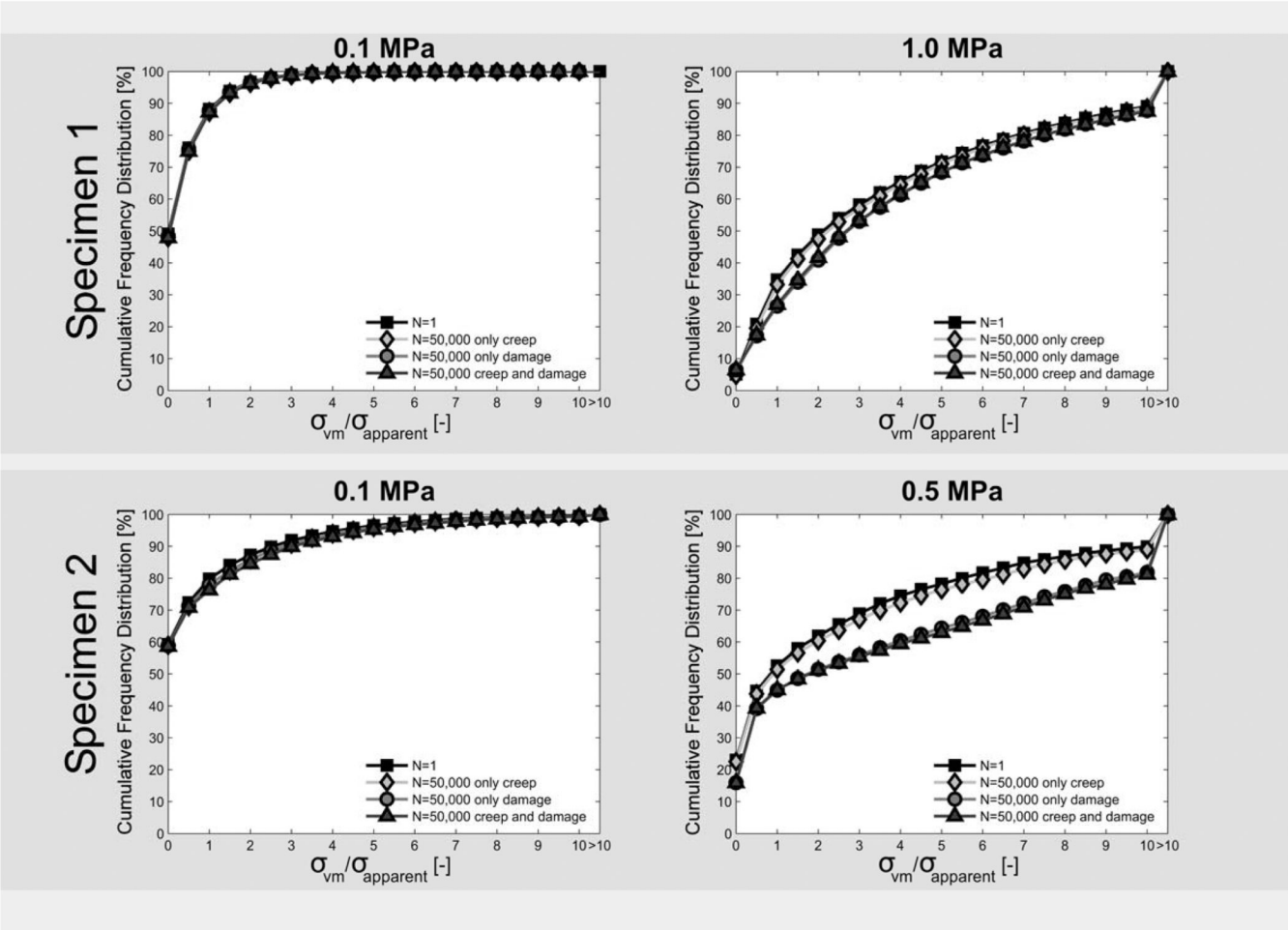

Figure 7.

Cumulative frequency distribution for $\frac{\sigma_{VM}}{\sigma_{app}}$ in the bone. When specimen 1 and specimen 2 were loaded to 0.1 MPa, the bone stress level hardly changed after 50,000 load cycles as a result of its deformation mode. When loaded to higher stress levels both specimens showed a decrease in low bone stresses, $\frac{\sigma_{VM}}{\sigma_{app}} \leq 1$. Furthermore, it shows that cement fatigue damage results in higher stresses in the bone and that cement creep has limited effect on the stress level.

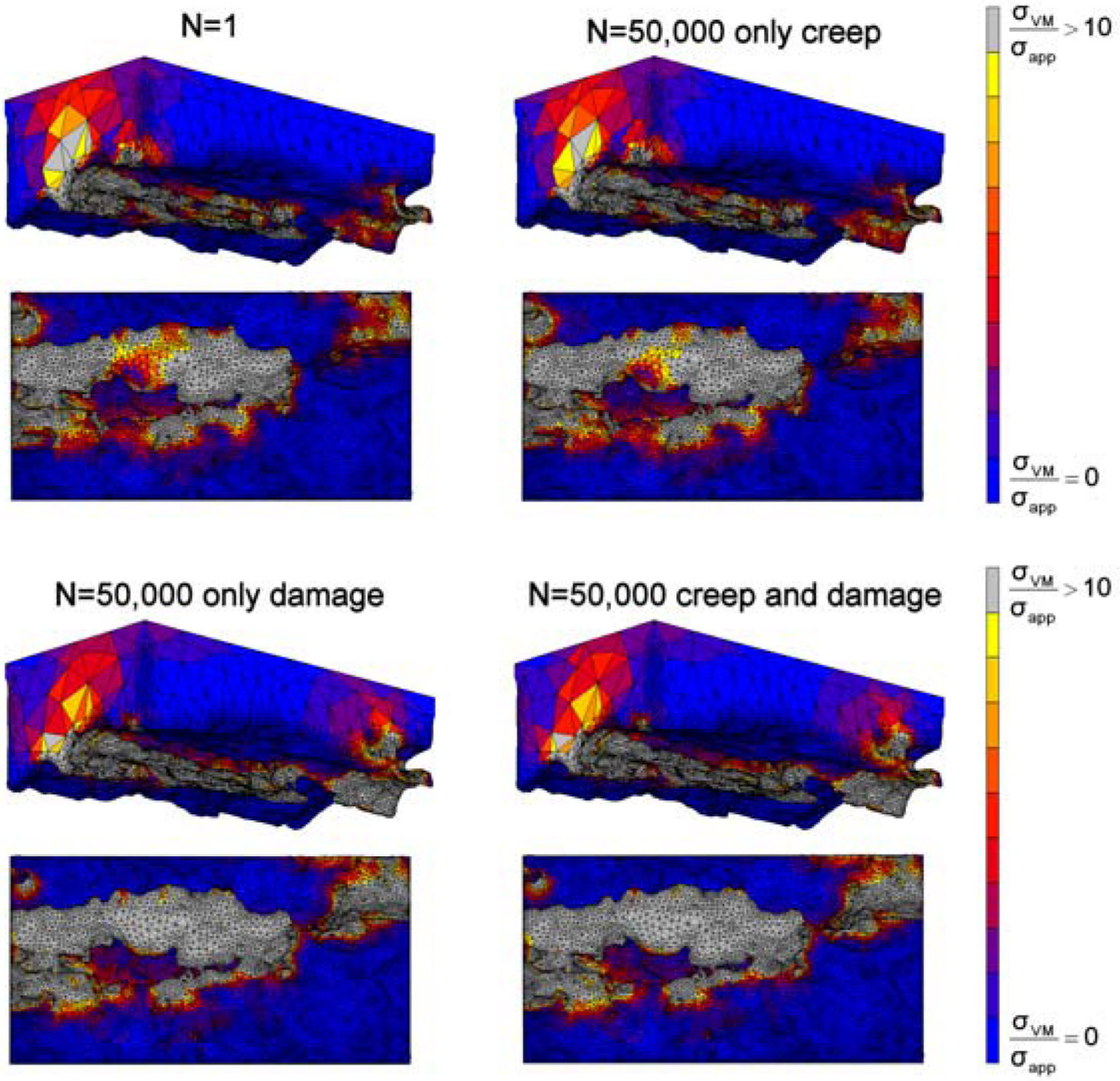

Figure 8.
Stress level patterns in the bone of specimen 2 loaded with 0.5 MPa.